The statistics of the vestibular input experienced during natural self-motion differ between rodents and primates

Jérome Carriot, Mohsen Jamali, Maurice J. Chacron 🆔 and Kathleen E. Cullen

Department of Physiology, McGill University, Montreal, QC, Canada

Key points

- In order to understand how the brain's coding strategies are adapted to the statistics of the sensory stimuli experienced during everyday life, the use of animal models is essential.
- Mice and non-human primates have become common models for furthering our knowledge of the neuronal coding of natural stimuli, but differences in their natural environments and behavioural repertoire may impact optimal coding strategies.
- Here we investigated the structure and statistics of the vestibular input experienced by mice *versus* non-human primates during natural behaviours, and found important differences.
- Our data establish that the structure and statistics of natural signals in non-human primates more closely resemble those observed previously in humans, suggesting similar coding strategies for incoming vestibular input.
- These results help us understand how the effects of active sensing and biomechanics will differentially shape the statistics of vestibular stimuli across species, and have important implications for sensory coding in other systems.

Abstract It is widely believed that sensory systems are adapted to the statistical structure of natural stimuli, thereby optimizing coding. Recent evidence suggests that this is also the case for the vestibular system, which senses self-motion and in turn contributes to essential brain functions ranging from the most automatic reflexes to spatial perception and motor coordination. However, little is known about the statistics of self-motion stimuli actually experienced by freely moving animals in their natural environments. Accordingly, here we examined the natural self-motion signals experienced by mice and monkeys: two species commonly used to study vestibular neural coding. First, we found that probability distributions for all six dimensions of motion (three rotations, three translations) in both species deviated from normality due to long tails. Interestingly, the power spectra of natural rotational stimuli displayed similar structure for both species and were not well fitted by power laws. This result contrasts with reports that the natural spectra of other sensory modalities (i.e. vision, auditory and tactile) instead show a power-law relationship with frequency, which indicates scale invariance. Analysis of natural translational stimuli revealed important species differences as power spectra deviated from scale invariance for monkeys but not for mice. By comparing our results to previously published data for humans, we found the statistical structure of natural self-motion stimuli in monkeys and humans more closely resemble one another. Our results thus predict that, overall, neural coding strategies used by vestibular pathways to encode natural self-motion stimuli are fundamentally different in rodents and primates.

Introduction

Understanding how sensory neurons transmit information about behaviourally relevant stimuli is a major challenge in system neuroscience. Growing evidence shows that neural coding strategies are adapted such as to optimize processing of stimuli occurring in the natural environment by taking advantage of their statistical structure (e.g. their probability of occurrence or their spectral frequency content; Attneave, 1954; Laughlin, 1981; Barlow, 2001; Simoncelli & Olshausen, 2001). As such, it is necessary to first understand natural stimulus statistics in order to make progress towards understanding the neural code. The prevailing view is that natural stimuli across sensory systems display probability distributions that deviate from normality due to characteristic long tails, indicating that high stimulus intensities are more likely to occur. Furthermore, natural stimuli display scale invariance (i.e. they are self-similar when observed at different temporal or spatial scales). As a result, their spectral power decays as a power law with increasing spatial or temporal frequency (reviewed in Simoncelli & Olshausen, 2001). Studies performed across systems have shown that the properties of sensory neurons optimize their coding of natural stimuli based on both probability of occurrence in the natural environment (Laughlin, 1981) as well as their spectral structure. For the latter, optimized coding can be achieved by decorrelating the sensory input: such 'temporal whitening' has been observed across systems and species and is thought to be achieved by ensuring a precise match between the tuning of sensory neurons and the statistics of natural stimuli (i.e. 'white'; Dan *et al.* 1996; Rodriguez *et al.* 2010; Huang *et al.* 2016). As a result, the neural response to natural stimulation will be independent of frequency. At the perceptual level, optimized coding of natural stimuli displaying scale invariance is thought to underlie Weber's law, which predicts that sensory discrimination thresholds are proportional to stimulus magnitude (Laming, 1986; Zanker, 1996; Dehaene, 2003; Brannon *et al.* 2008; Francisco *et al.* 2008). However, to date it remains largely unknown whether coding strategies used in the vestibular system, which contributes to essential brain functions ranging from stabilization of gaze, control of balance and posture to spatial perception and motor coordination, are adapted to natural self-motion statistics. This is in part due to the fact that recent experiments have demonstrated that the statistical structure of natural vestibular stimuli experienced by human subjects display power spectra that are not well fitted by a power law as a result of pre-neuronal filtering (Carriot *et al.* 2014); specifically, motor control and biomechanics shape the statistics of natural vestibular stimuli before neural processing. Furthermore, most studies of vestibular processing have used artificial (e.g. sinusoidal or noise) stimuli (reviewed in Cullen, 2012).

In order to understand whether and, if so, how vestibular neural coding strategies are adapted to the statistics of stimuli in the natural environment, it is useful to compare results obtained across multiple species. This is because such a comparative approach allows one to distinguish neural coding strategies that are common across species from those that are species-specific. On the one hand, there are clear similarities between morpho-physiological properties underlying vestibular signal processing across vertebrates, implying common strategies of sensory processing across species (reviewed in Straka *et al.* 2016). On the other hand, several studies have uncovered important differences in the response properties of vestibular neurons across species (e.g. see discussions in Beraneck & Cullen, 2007; Medrea & Cullen, 2013), suggesting that neural coding strategies are species specific, which could result from differences in natural self-motion statistics. However, no study to date has systematically compared the statistical properties of natural self-motion stimuli across species.

To this end, we investigated the structure of natural self-motion signals experienced by mice and monkeys during natural behaviours and compared them to existing data from human subjects. Notably, non-human primates have become a standard model for furthering our knowledge of basic vestibular processing and advancing translational research due to their evolutionary proximity to humans. Further, recent advances in the generation of mouse lines with defined genetic backgrounds and/or transgenic lines, such as CRE, combined with viral-based optogenetics have provided new opportunities to probe the functional circuitry of vestibular pathways (e.g. Vidal *et al.* 2004; Alagramam *et al.* 2005; Hoebeek *et al.* 2005; Bagnall *et al.* 2007; McElvain *et al.* 2010; Schlecker *et al.* 2011; Jones & Jones, 2014; Luebke *et al.* 2014). Mice and monkeys are thus two important animal models that are used to uncover vestibular neural coding strategies.

Our results reveal that there are important differences between the statistical properties of natural self-motion stimuli across species. Notably, self-motion generated larger intensity vestibular stimuli in monkeys than in mice. Furthermore, while motion in all six dimensions deviated from normality due to relatively long tails, demonstrating that self-motion was most often relatively low intensity in both species, there were characteristic differences in the spectral power of sensory inputs. First, our analysis of natural rotational stimuli revealed that while stimuli were not scale invariant in either species, in monkeys power spectra decreased more slowly for low and more sharply for high temporal frequencies, with the transition frequencies (2–10 Hz) similar to those previously reported for humans (Carriot *et al.* 2014). Qualitatively similar results were obtained for mice. Notably, this unique structure differs

from the natural spectra of other sensory modalities which show a power-law relationship with frequency, indicating spectral scale invariance. Furthermore, our analysis of natural translational stimuli also demonstrated marked differences between species. While the associated spectra for monkeys decreased more slowly for low and more sharply for high temporal frequencies (i.e. were not scale invariant, as is also the case for humans, Carriot *et al.* 2014), the associated spectra for mice did follow a power law and thus were scale invariant. Accordingly, we conclude that the statistics of incoming natural vestibular stimuli differ significantly in mice and monkeys, with the statistics for monkeys more closely resembling those observed previously in humans (Carriot *et al.* 2014). In turn, we speculate that these differences in natural stimuli drive complementary differences in the neural coding strategies between species.

Methods

Animals

Five male 129SvEv adult mice (∼30 g) and two male macaque monkeys (*Macaca fascicularis*) were included in this study. All experimental protocols were approved by the McGill University Animal Care Committee and all procedures were carried out in strict compliance with the guidelines of the Canadian Council on Animal Care.

Head movement recordings in mice

Head movements were recorded in mice using a micro-electromechanical systems (MEMS) module (LSM330DLC, 4 × 4.5 × 1 mm), which combined three linear accelerometers (recording linear accelerations along the fore–aft, inter-aural and vertical axes) and three gyroscopes (recording angular velocity about pitch, roll and yaw). This MEMS module was firmly secured to a stainless steel head-post implanted on top of the animals' skull.

The surgical procedures and anaesthesia protocols for head-post implantation were as has been described previously (Beraneck & Cullen, 2007; Medrea & Cullen, 2013). Briefly, mice were anaesthetized with an intramuscular injection of a mixture of atropine (5 × 10^{-4} mg g^{-1}), ketamine (10^{-1} mg g^{-1}), acepromazine maleate (2 × 5.10^{-2} mg g^{-1}), xylazine (10^{-1} mg g^{-1}), and sterile saline. During surgery the small stainless-steel post was chronically fastened to each animal's skull with dental acrylic. After the surgery, animals were kept in isolated cages and closely monitored during the first 48 h. Buprenorphine (0.05 mg kg^{-1}) was utilized for postoperative analgesia, and xylocaine (2%, Astra Pharma, ON, Canada) was applied to the incision site. In addition, care was provided to avoid hypothermia and dehydration.

Note that the head-post was implanted at the Bregma landmark and was oriented such that in resting posture (Vidal *et al.* 2004) the plane spanned by the fore–aft and inter-aural axes of the MEMS module was set parallel to the earth horizontal plane.

Each mouse was placed separately into a large open arena (75 cm diameter) containing familiar bedding as well as food pellets strewn at random spots and was allowed to explore the environment and interact with another mouse from its home cage for 30 min. The repertoire of the exploring behaviours consisted of: walking/running around, foraging, sniffing, grooming, eating food, and climbing up the arena's walls. The data from the six sensors were sampled at 100 Hz and recorded on a microSD card. Subsequent to completing these experiments, all animals were assigned to an on-going neurophysiological study.

Head movement recordings in monkeys

Experiments were performed with two rhesus monkeys (*Macaca mulatta*) that were sourced from World Wide Primates, where they inhabited large outdoor group enclosures for the first 3–4 years of their lives. In addition, at McGill they had daily access to the large 'playspace' within the animal resources center (8 feet high 6 feet wide by 17 feet deep).

The monkeys were prepared for recording experiments using aseptic surgical techniques. Fifteen minutes preoperatively and every 2.5–3 h during surgery, animals were injected with the anticholinergic glycopyrrolate (0.005 mg kg^{-1} I.M.) to stabilize heart rate and to reduce salivation. Animals were then pre-anaesthetized using ketamine hydrochloride (15 mg kg^{-1} I.M.). Finally, buprenorphine (0.01 mg kg^{-1} I.M.) and diazepam (1 mg kg^{-1} I.M.) were injected as an analgesic and to provide muscle relaxation, respectively. Loading doses of dexamethasone (1 mg kg^{-1} I.M.) and cefazolin (50 mg kg^{-1} I.V.) were administered to reduce swelling and prevent infection, respectively. Surgical levels of anaesthesia were then achieved using isoflurane gas, maintained at 0.8–1.5%, together with a minimum 3 l min^{-1} (dose adjusted to effect) of 100% oxygen. Heart rate, blood pressure, respiration and body temperature were monitored throughout the procedure. During surgery, a stainless-steel post, which allowed fixation of the MEMS sensor to the animal's head during experiments, was chronically fastened to each animal's skull with stainless-steel screws and dental acrylic. After surgery, dexamethasone (0.5 mg kg^{-1} I.M.; for 4 days) administration was continued. Buprenorphine (0.01 mg kg^{-1} I.M.) was given as postoperative analgesia every 12 h for 2–5 days, depending on the animal's pain level, and anafen (2 mg kg^{-1} and then 1 mg kg^{-1} on subsequent days) was used as an anti-inflammatory. In addition, cefazolin (25 mg kg^{-1}) was injected twice daily for 10 days.

Animals recovered for 2 weeks before any experimenting began.

Following a recovery period of at least 1 month, head movement recordings were then made using a micro-electromechanical systems (MEMS) module (iNEMO platform, STEVAL-MKI062V2; STMicroelectronics). The MEMS module, a battery, and a microSD card were encased in a light (64 g) and small (35 × 35 × 15 mm) enclosure, which was firmly secured to the head posts of two macaque monkeys. Specifically, the plane spanned by the fore–aft and lateral axes of the MEMS module was set parallel to the horizontal stereotaxic plane (i.e. the plane passing through the inferior margin of the orbit and the upper margin of the external auditory meatus; Carriot *et al.* 2014). Data from each of the six sensors were sampled at 100 Hz and recorded wirelessly on a microSD card. The dataset was the same as that previously published (Schneider *et al.* 2015); however, we note that Schneider *et al.* (2015) did not consider the spectral content of the recorded signals.

Each monkey was released separately into a large expansive space (240 m³) where it was able to freely move and interact with another monkey from our colony for 160 min while a camera was recording its behaviour. Enrichment materials (scattered treats, toys, etc.) as well as multiple structures that the monkeys could climb, were distributed throughout this space. We note that similar statistics were observed when monkeys were released into a smaller enclosure (9.5 m³), suggesting that the size of the environment does not strongly influence stimulus statistics. Naturally generated behaviours included activities with high levels of activity such as walking, running, jumping and climbing, and rapid head movements, as well as activities with lower levels of activity such as foraging, holding and playing with objects, grooming, and simply sitting and observing the environment. Subsequent to completing these experiments, both animals were assigned to an on-going neurophysiological study.

Data analysis

The angular velocity data recorded from the gyroscopes were projected onto the semi-circular canal planes (left anterior-right posterior: LARP, right anterior-left posterior: RALP and horizontal: YAW) using the rotation matrix:

$$\begin{pmatrix} v_{\text{LARP}} \\ v_{\text{RALP}} \\ v_{\text{YAW}} \end{pmatrix} = \begin{bmatrix} \cos(\theta) & -\sin(\theta) & 0 \\ \sin(\theta) & \cos(\theta) & 0 \\ 0 & 0 & 1 \end{bmatrix}$$
$$\times \begin{bmatrix} \cos(\gamma) & 0 & -\sin(\gamma) \\ 0 & 1 & 0 \\ \sin(\gamma) & 0 & \cos(\gamma) \end{bmatrix} \begin{pmatrix} v_x \\ v_y \\ v_z \end{pmatrix},$$

with $\theta = 45$ deg and $\gamma = 15$ deg for mice (Vidal *et al.* 2004) and 22 deg for monkeys (Sadeghi *et al.* 2009).

Power spectral densities (PSD function in Matlab, the Mathworks, Natick, MA, USA) were obtained using Welch's average periodogram. Probability distributions were obtained using binwidths of 0.01 G ($G = 9.8$ m s⁻²) and 10 deg s⁻¹ for linear acceleration and angular velocity, respectively. Deviation from normality was quantified by the excess kurtosis (K) defined as:

$$K = \frac{\langle (X - \mu)^4 \rangle}{\sigma^4} - 3,$$

where μ and σ are the mean and standard deviation of the data X, respectively, and $< \cdots >$ is the average.

We fitted the power spectrum with a power law over both the low and high frequency ranges. The low frequency range was set from 0.05 to 2 Hz, while the high frequency range was set from 10 to 30 Hz. The power spectra was always above the MEMS module's noise level, which was determined by recording signals for 15 m while the MEMS module was not moving. The transition frequency was determined as the frequency at which the two power-law fits intersect.
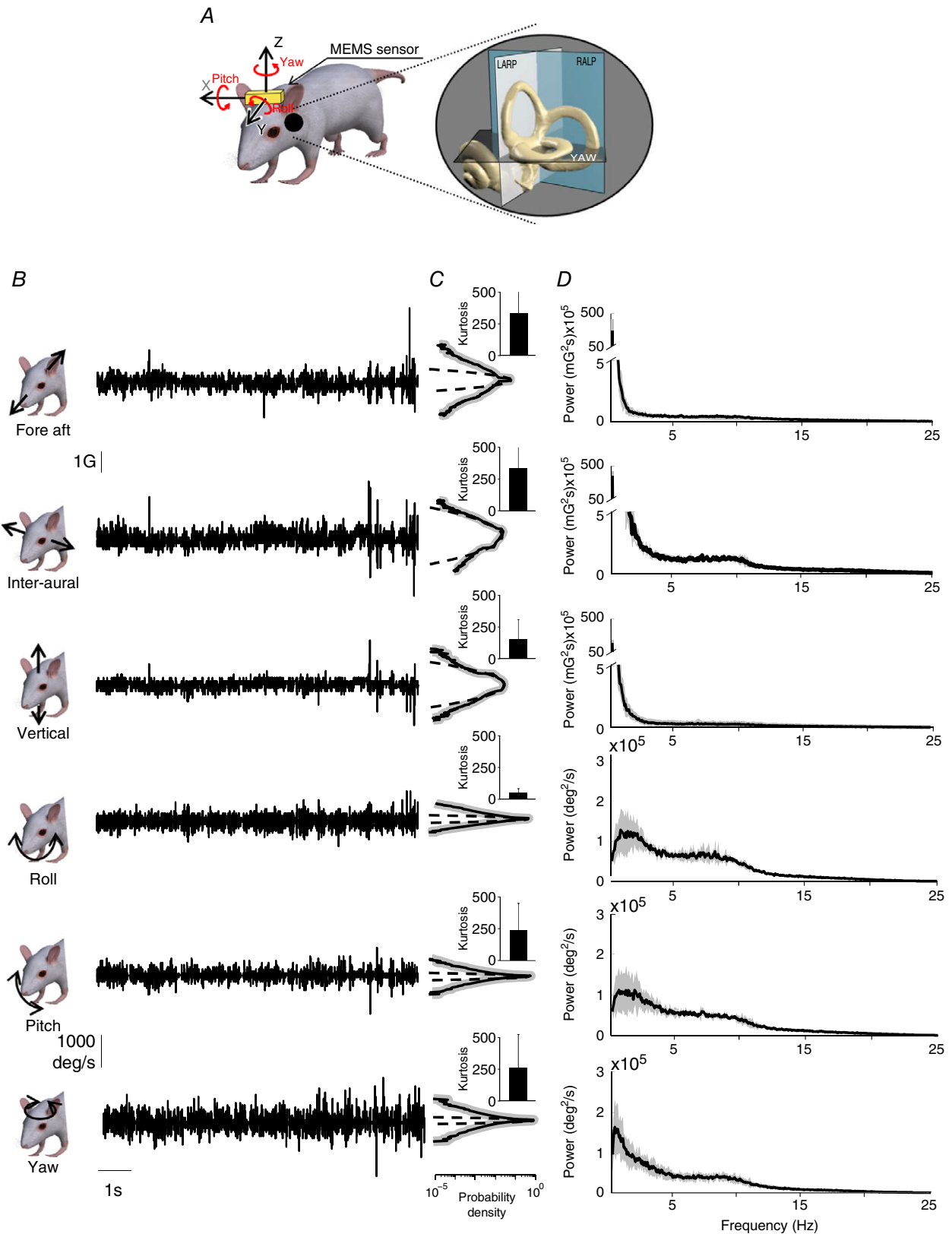
Statistical significance was determined using a Wilcoxon rank sum test. Results are reported (and plotted) as means ± S.E.M. and the level of statistical significance was set at $P < 0.05$.

Results

Statistics of natural self-motion signals in mice

We first characterized the natural statistics of vestibular stimulation experienced by mice during natural everyday behaviours (e.g. walking, running, foraging, grooming, eating, climbing, etc.). Measurements of stimuli along six axes of translational and rotational motion were made using an extremely lightweight MEMS module (see Methods and Fig. 1A) that was attached to the head (Fig. 1A). Angular velocity signals were projected onto each animal's semicircular canal planes (LARP, RALP, and YAW) prior to analysis (see Methods), in order to describe the statistical properties of stimuli activating each of the three semicircular canals.

The time varying profiles and statistics of vestibular signals measured in each of the three axes of translation and three axes of rotation are shown in Fig. 1B and C. The intensity of these stimuli could reach up to 1300 deg s⁻¹ and 4.5 G of angular velocity and linear acceleration, respectively (Fig. 1B). Furthermore, we found that the probability distributions of vestibular stimuli (angular velocity or linear acceleration) in all six-motion dimensions were not Gaussian (compare dashed and continuous lines, Fig. 1C), but instead where characterized by large (>10) positive excess kurtosis

Figure 1. Statistics of mouse natural vestibular stimuli

A, representation of a mouse with the MEMS module (gold box). The inset shows a magnified image of the vestibular sensors and the corresponding semi-circular canal planes. *B*, a 10 s example of fore–aft acceleration (first

values (Fig. 1*C*, insets). Specifically, the distributions decayed more slowly than a Gaussian (Fig. 1*C*, compare continuous and dashed lines). This implies that stimuli with high intensities were more likely to occur. Overall, the population-averaged excess kurtosis values were significantly different from zero ($P < 0.01$ for all axes).

We next computed the power spectra of the self-motion signals generated by mice during natural behaviour as a function of temporal frequency (Fig. 1*D*). Quantification of our results are shown in the log–log plots of Fig. 2*A*. First, we found that the spectra of translational movements generated during natural behaviours in the mouse were well fitted by a power law for all three axes (Fig. 2*A*, left panels). In contrast, the spectra of rotational movements were not well fitted by a power law (Fig. 2*A*, right panels). Instead these spectra were relatively flat at lower frequencies (i.e. $< \sim$10 Hz, red line) and then decreased sharply for higher frequencies (i.e. $> \sim$10 Hz, blue line). Consequently, the exponent of the best power-law fit obtained over the low frequency range (which corresponds to the slope of the fit on a log–log plot) was less than the exponent of the best power-law fit obtained over the high frequency range (Fig. 2*A*). To quantify this effect, we compared the slopes obtained for the low (Fig. 2*B*, grey bars) and high (Fig. 2*B*, black bars) frequency ranges. We found that these were comparable for all three axes of translation ($P > 0.1$), but significantly different from each other for all three axes of rotation ($P < 0.01$). Finally, for each axis of rotation, we computed the frequency at which both power-law fits intersected (i.e. the 'transition frequency') and found that on average this measure ranged from ~7 to 10 Hz (Fig. 2*C*).

Statistics of natural self-motion signals in monkeys

Primate posture and locomotion are characterized by distinctive features including protracted forelimb posture, powerful pedal grasping, hind limb dominance and diagonal sequence of footfalls (reviewed in Schmidt, 2008), which differs from other mammals. Accordingly, we posited that natural vestibular signals resulting from self-motion would differ between mice and monkeys. To address this important hypothesis, we next characterized the natural statistics of vestibular stimulation experienced by monkeys during natural everyday behaviours (e.g. walking, running, foraging, grooming, eating, climbing, etc.). Measurements of stimuli along six axes of translational and rotational motion were made using a portable

MEMS module that was attached to the subject's head (see Methods and Fig. 3*A*). Angular velocity signals were then projected onto each animal's semicircular canal planes (see Methods), in order to describe the statistical properties of stimuli activating each of the three semicircular canals.

The time varying profiles and statistics of vestibular signals measured in each of the three axes of translation and three axes of rotation are shown in Fig. 3*B* and *C*. The intensity of these stimuli could reach up to 1500 deg s^{-1} and 8 *G* of angular velocity and linear acceleration, respectively (Fig. 3*B*). Furthermore, we found that the probability distributions of vestibular stimuli (angular velocity or linear acceleration) in all six-motion dimensions were not Gaussian (compare dashed and continuous lines, Fig. 3*C*), but instead were characterized by long tails, as quantified by large (>10) positive excess kurtosis values (Fig. 3*C*, insets), indicating that higher intensities were more likely to occur. Overall, the population-averaged excess kurtosis values were significantly different from zero ($P < 0.01$ for all axes).

Figure 3*D* illustrates the power spectra of the self-motion signals generated by monkeys during natural behaviour on a linear scale. To determine whether the spectra of either translational or rotational movements were well fitted by a power law, we plotted these same data on a logarithmic scale. In contrast to our above findings in mice, translational movement was generally not well fitted by a power law (Fig. 4*A*, left); only vertical motion was well fitted by a power law over the entire frequency range. Similar to mice, we further found that rotational movement was not well fitted by a power law in all three-motion dimensions (Fig. 4*A*, right). Thus, overall for all but vertical translations, spectra decayed slowly for lower frequencies and more sharply for higher frequencies (Fig. 4*A*, difference in slope indicated by red arrows). Consequently, the best power-law fit obtained over the low frequency range gave rise to a different exponent (which corresponds to the slope of the fit on a log–log plot) from the best power-law fit obtained over the high frequency range (Fig. 4*A*). Again to quantify this effect, we compared the slopes obtained for the low (Fig. 4*B*, grey bars) and high (Fig. 4*B*, black bars) frequency ranges. We found that these were significantly different from each another for all axes of motion with the exception of vertical translational motion ($P < 0.05$). Finally, for fore–aft and inter-aural translational motion and each axis of rotation, we computed the frequency at which both power-law fits intersected (i.e. the 'transition frequency') and found values between ~2 and
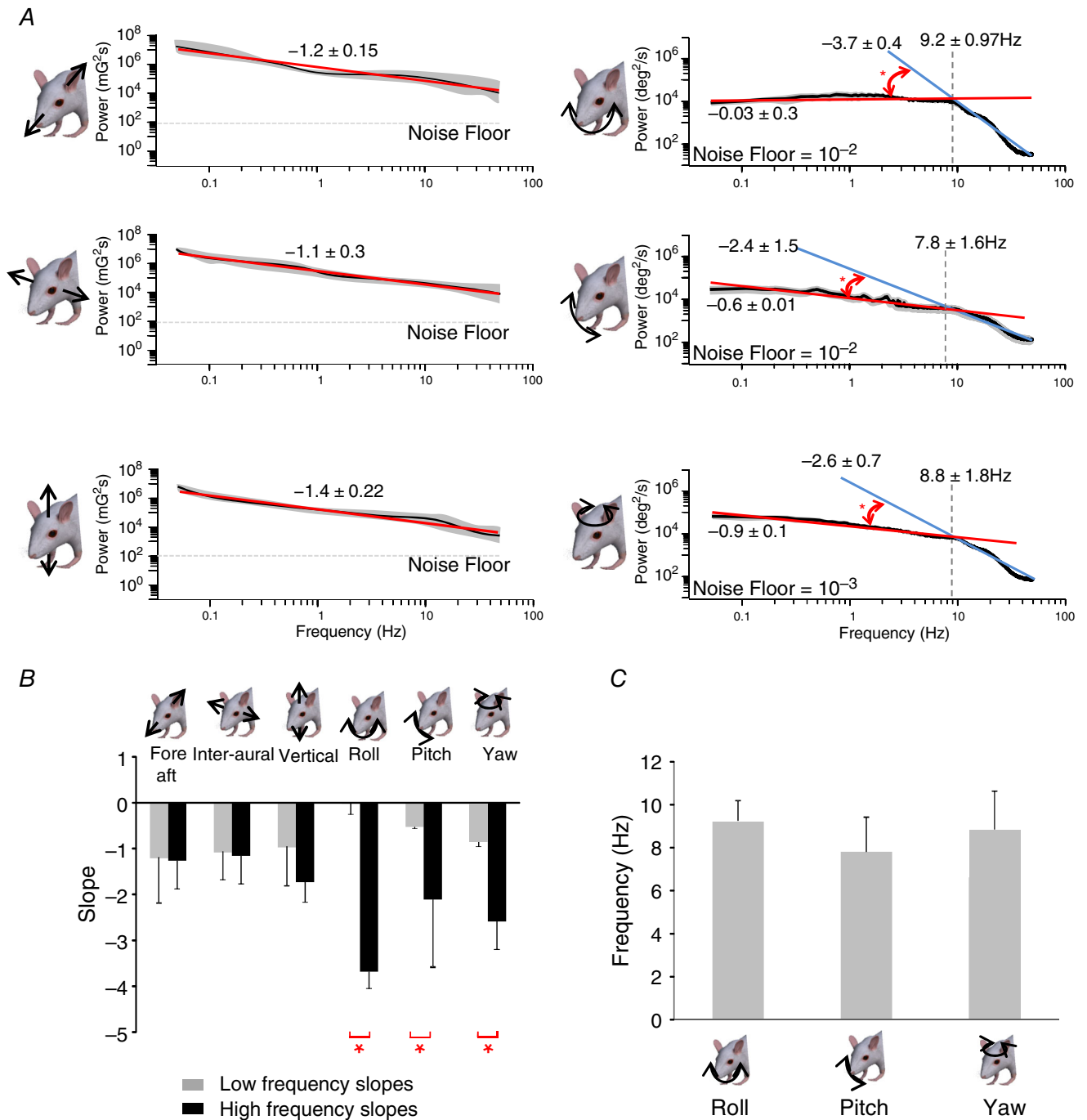
Figure 2. Natural mouse head rotation did not follow a power law

A, power spectra on a log–log scale for the 6 motion dimensions and power-law fits over the low (0.05–2 Hz, red) and the high (10–30 Hz, blue) frequency ranges. The power-law exponents (i.e. slopes) and the transition frequencies (i.e. the frequency at which the power-law fits intersect) are also shown. B, population-averaged slopes obtained for the low frequency range (grey bars) were significantly different from those obtained for the high frequency range (black bars) only for rotations at the $P = 0.05$ level (*). C, population-averaged transition frequencies for three rotational dimensions ($P = 0.31$, Kruskal Wallis test).
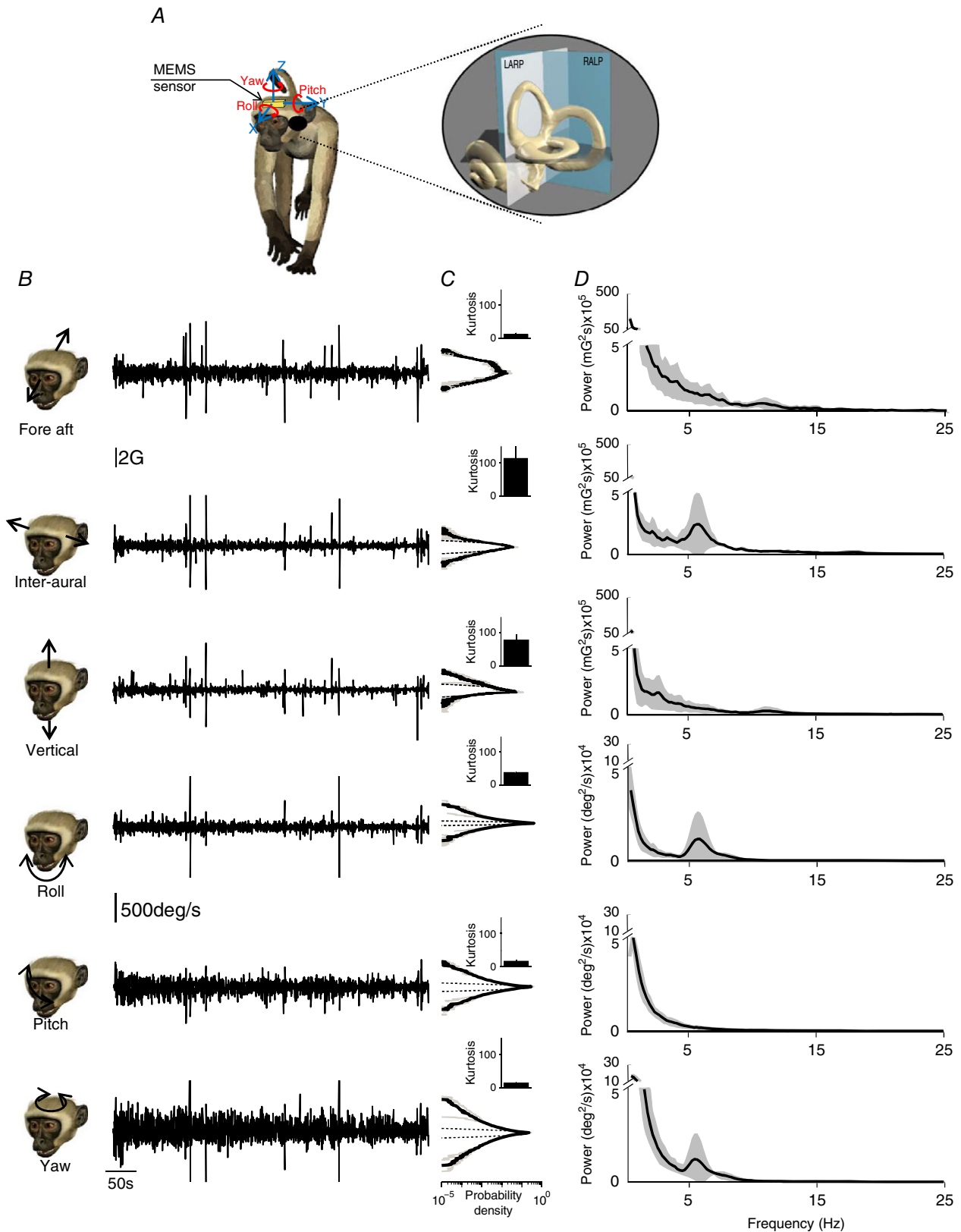
Figure 3. Statistics of monkey natural vestibular stimuli
A, representation of a monkey wearing the MEMS module (gold box). The inset shows a magnified image of the vestibular sensors and the corresponding semi-circular canal planes. *B*, fore–aft acceleration (first row),

inter-aural linear acceleration (second row), vertical linear acceleration (third row), LARP angular velocity (Roll, fourth row), RALP angular velocity (Pitch, fifth row) and yaw angular velocity (sixth row) signals during different everyday activities. *C*, population-averaged probability distributions for these signals (continuous black lines) with corresponding standard deviation (shaded areas) and best Gaussian fit (dashed lines). Inset: population-averaged excess kurtosis values. *D*, population-averaged power spectra (black) of these signals with corresponding standard deviations (dark grey bands). The bumps evident at 5–7 Hz in the inter-aural, roll and yaw axes are due to rhythmic activities such as walking and running, and are observed at lower frequencies in humans (∼2 Hz; Carriot *et al.* 2014).

10 Hz (Fig. 4*C*). Taken together, our results demonstrate that during natural behaviours, the power spectra of translational or rotational self-motion signals experienced by non-human primates are not well fitted by a power law.

Comparison between the statistics of natural self-motion signals experienced by mice, monkeys and humans

In order to understand whether there are differences in the statistics of natural vestibular signals experienced across species, we next directly compared the head motion signals generated during self-motion in mice and monkeys, and those previously published for humans (Carriot *et al.* 2014). This comparison is illustrated in Fig. 5, where the power spectra of natural vestibular stimuli are superimposed in each panel (i.e. Fig. 5*A–F*) for all six motion dimensions for mice (red), monkeys (green) and humans (blue). Notably, the relative percentage of head motion at higher frequencies was significantly higher for mice than for monkeys or humans in all rotational and translational axes (Fig. 5, insets; $P < 0.005$). For translations, power spectra obtained for mice were well fitted by power laws whereas this was not the case for monkeys and humans (Fig. 5*A*, *C* and *E*). For rotations, the power spectra obtained for mice in general decayed more slowly in that they displayed more power over the high (>10 Hz) frequency range than the power spectra obtained for monkeys and humans (Fig. 5*B*, *D* and *F*). A comparison of the transition frequencies for translations (i.e. the frequency at which the power spectra starts decaying more sharply) revealed no significant ($P > 0.5$) difference between humans and monkeys for fore–aft and inter-aural motion. Transition frequencies for rotation were significantly different between humans, monkeys and mice ($P < 0.05$), and humans had consistently lower transitions values in the roll and yaw axes.

Comparing the power-law exponents obtained for the low and high frequency ranges provided further confirmation that natural vestibular stimuli display significant differences across all three species (Fig. 6). While the power-law exponents over the low frequency range were similar, power-law exponents over the high frequency range tended to be highest in humans and lowest in mice (Fig. 6, compare blue and red bars). Power-law exponents over the high frequency range in monkeys were,

in general, between those observed for mice and humans (Fig. 6, compare green, red and blue bars), with a notable exception for roll. Thus, natural vestibular stimuli tended to deviate most from scale invariance in humans, followed by monkeys, and deviated the least or not at all in mice.

We conclude that, while the statistics of incoming natural vestibular stimuli differ significantly between all three species, those experienced by monkeys were more similar to humans than those experienced by mice. We discuss the possible causes for these differences as well as their implication for sensory processing below.

Discussion

In the present study we measured, for the first time, the statistics of self-motion signals experienced by mice and monkeys during natural behaviours and found important differences. While in both species probability distributions were not Gaussian but were instead characterized by long tails as quantified by large and positive excess kurtosis values across all six motion dimensions, the vestibular stimuli experienced by monkeys reached larger intensities than those in mice (1500 deg s^{-1} and 8 G *versus* 1300 deg s^{-1} and 4.5 G, respectively). Significant differences were also observed in spectral content. Specifically, for monkeys, spectral frequency content of translational stimuli decreased relatively slowly over low ($< \sim 10$ Hz) and more rapidly over high frequency ranges whereas the rate of decay was relatively constant across frequencies for mice. A comparison between our results and those obtained previously in humans revealed that vestibular stimuli experienced during natural self-motion by monkeys were more similar to humans than those experienced by mice. Taken together, our analysis revealed that statistics of natural vestibular stimuli experienced by rodents and primates display differences in their structure, suggesting that the neural coding strategies used to process natural self-motion stimuli differ in both orders of species.

Natural vestibular stimuli deviate from scale invariance across species

Our above results show that natural rotational vestibular stimuli in both mice and monkeys are characterized by power spectra that do not decrease as a power law with increasing temporal frequency. Instead, spectral
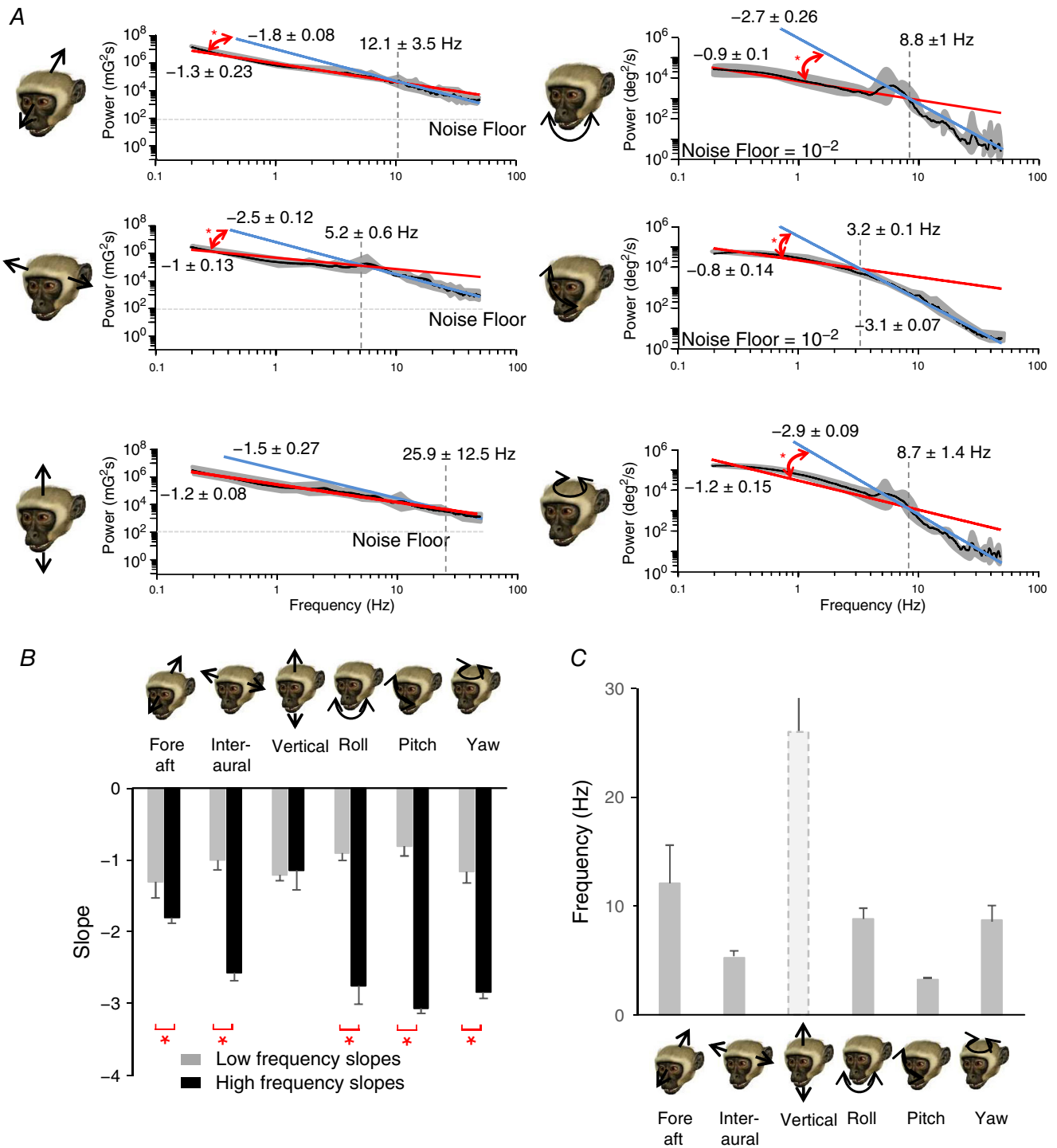
Figure 4. Monkey natural vestibular stimuli did not follow a power law
A, power spectra on a log–log scale for the 6 motion dimensions and power-law fits over the low (0.05–2 Hz, red) and the high (10–30 Hz, blue) frequency ranges. The power-law exponents (i.e. slopes) and the transition frequencies (i.e. the frequency at which the power-law fits intersect) are also shown. *B*, population-averaged slopes obtained for the low frequency range (grey bars) were significantly different from those obtained for the high frequency range (black bars) at the $P = 0.05$ level (*). *C*, population-averaged transition frequencies for all six dimensions ($P = 0.07$, Kruskal Wallis test).
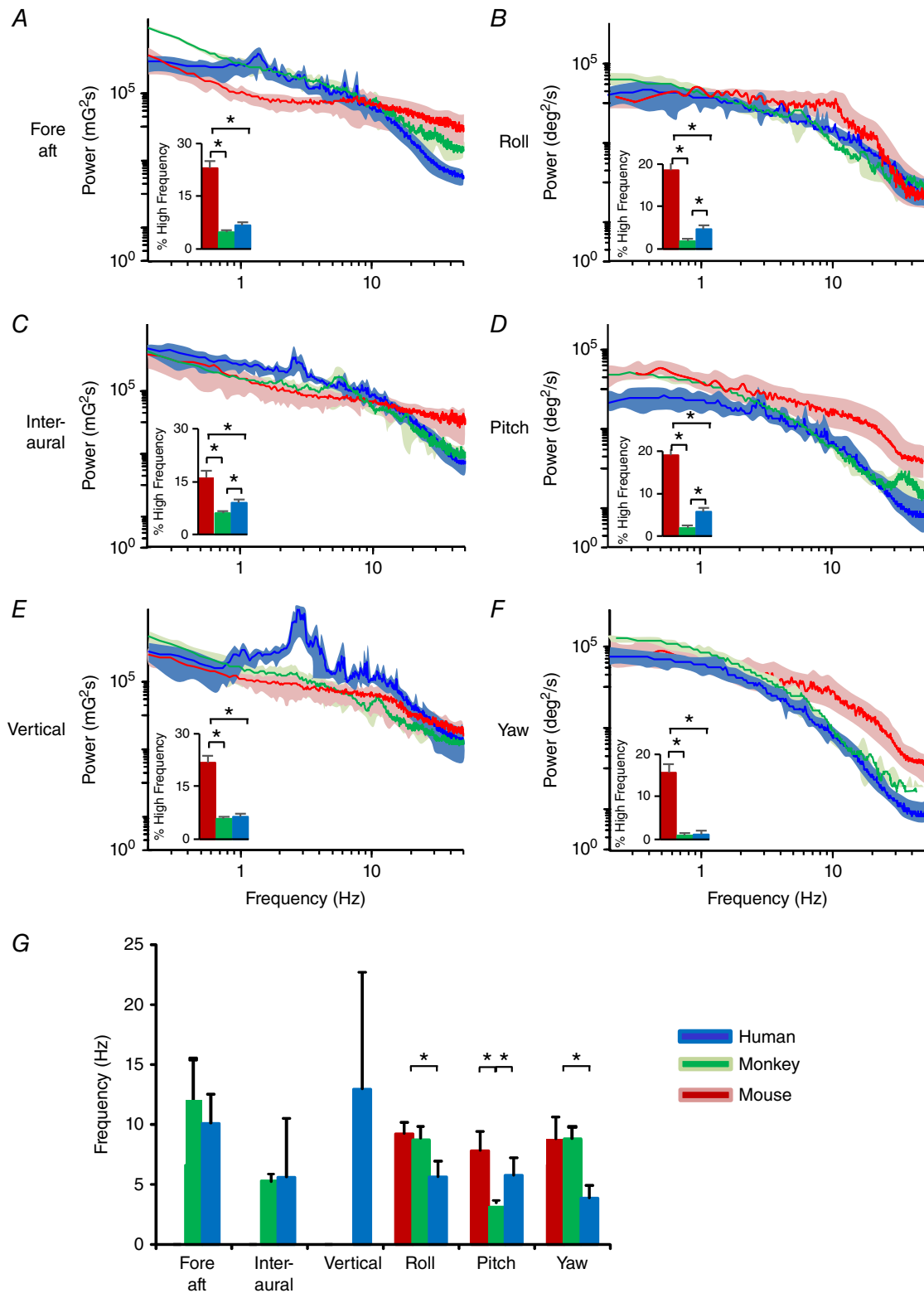
Figure 5. Comparison of natural self-motion signals in the mouse, monkey and human
A–F, power spectra on a log–log scale for the six motion dimensions and standard deviation (shaded areas). *G*, population-averaged transition frequencies for all six dimensions. Inset: comparison of the percentage of motion observed at higher frequencies (>7 Hz) across species.

power decreases more rapidly at higher than at lower frequencies. Thus, contrary to results obtained in other sensory systems (Simoncelli & Olshausen, 2001), natural rotational vestibular stimuli in mice and monkeys do not display scale invariance. In addition, we found important differences between the natural translational vestibular stimuli resulting from self-motion in mice and monkeys. Indeed, while stimuli experienced by the former deviated from scale invariance, those experienced by the latter did not. These results imply that different coding strategies are needed to optimally encode natural translational self-motion stimuli in monkeys and mice. Interestingly, a recent study of natural vestibular stimuli in humans has shown that both rotational and translational signals deviate from scale invariance (Carriot *et al.* 2014). Notably, both biomechanical filtering by the human body (McMahon, 1984; Zatiorsky, 1998; Nigg & Liu, 1999; Wakeling *et al.* 2002,2003; Hinz *et al.* 2010) and the behavioural repertoire (e.g. active behaviours such as walking) shape the frequency content of motion signals transmitted to the head (Carriot *et al.* 2014). In this context, differences between biomechanical filtering and behavioural repertoires for mice and monkeys will likely differentially shape the structure of natural vestibular signals reaching the vestibular organs prior to sensory transduction. It is furthermore likely that the observed similarities between natural self-motion stimulus statistics in human and non-human primates are the result of their more similar posture and locomotion as compared to rodents.

Neural coding strategies and natural stimulus statistics

Our results have important implications for understanding how natural vestibular stimuli are processed in the brain. Studies of other sensory systems have led to the view that the coding strategies used by sensory systems are adapted to optimally process natural stimuli (Attneave, 1954; Barlow *et al.* 1972; Simoncelli & Olshausen, 2001; Huang *et al.* 2016), such that sensory neurons transmit more information about natural stimuli than artificial ones (Rieke *et al.* 1995; Lewen *et al.* 2001; Machens *et al.* 2001; Vinje & Gallant, 2002). Theory has shown that optimized processing of stimuli requires a match between stimulus statistics and neuronal response properties (Laughlin, 1981; Rieke *et al.* 1995). In particular, neuronal responses to natural stimuli should display probability distributions that are independent of the stimulus (Laughlin, 1981) or power spectra that are independent of frequency (i.e. 'white'; Rieke *et al.* 1995). Experimental results have shown that both strategies
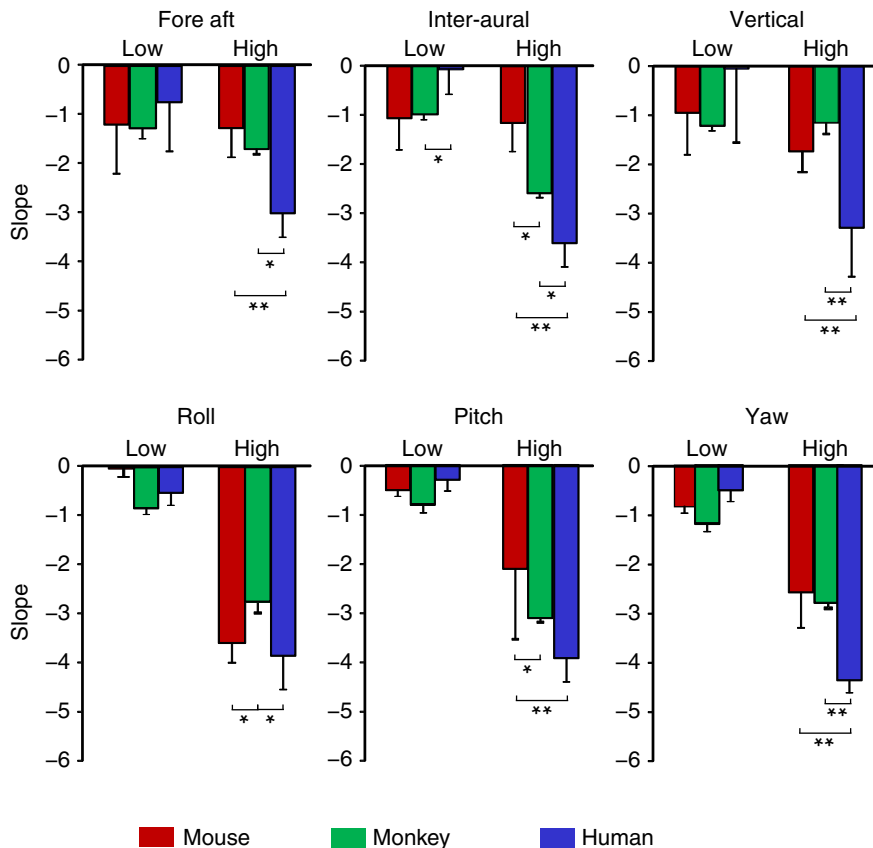
Figure 6. Comparison of mouse, monkey and human natural head motion slopes obtained for the low frequency range *versus* high frequency range
Slopes obtained for high frequency range signals were generally higher for monkeys (green) than mouse (red) and higher for human (blue) than monkey. *Significant difference at $P = 0.05$; **significant difference at $P = 0.001$.

are implemented across multiple systems and species (Laughlin, 1981; Dan *et al.* 1996; Alonso *et al.* 2004; Wark *et al.* 2007; Rodriguez *et al.* 2010; Pozzorini *et al.* 2013; Huang *et al.* 2016). Our results showing that natural self-motion stimuli display power spectra that deviate from scale invariance have important implications for coding. This is because the neural coding strategies used to optimally encode scale invariant stimuli will be different from those used to optimally encode stimuli that are not. Our findings therefore suggest that the coding strategies used by the vestibular system to encode natural self-motion differ significantly from those used by other sensory systems, where natural stimuli are instead scale invariant.

There is growing evidence that during evolution the vestibular end organs have adapted to the statistics of natural stimuli. In particular, there is a positive correlation between semicircular canal dimensions and body mass (Watt, 1924; Jones & Spells, 1963; Spoor *et al.* 1994, 2002), leading to the common view that increased sensitivity of larger semicircular canals ensures that more massive animals benefit from more accurate measurement of their slower movements (Jones & Spells, 1963; Graf *et al.* 1995; Alonso *et al.* 2004; Clarke, 2005). However, once body size is accounted for, it is notable that mammalian species with more rapid locomotion (e.g. non-human primates) have even larger canal arc sizes than those with slower locomotion (Spoor *et al.* 2007), suggesting that the vestibular system further evolved across mammalian species to efficiently process natural stimuli with different statistics.

We further found that the rotational vestibular stimuli experienced by monkeys reached larger intensities than those in mice. The comparison of the sensitivity of vestibular semicircular canal afferents in mice *versus* monkeys is consistent with this idea. On average, mouse afferents are three to four times less sensitive to head velocity relative to those of monkeys (i.e. compare Sadeghi *et al.* 2007 and Lasker *et al.* 2008). Similarly, afferent target neurons in the central vestibular nucleus also show relatively low sensitivities to both head velocity and eye position in mouse compared to monkey (Cullen *et al.* 1993; Cullen & McCrea, 1993). One possible explanation for the lower vestibular sensitivity in mice is that it could extend the linear range over which head movement is encoded. However, this does not seem likely. While the head of the mouse has less inertial load than that of larger species, thereby allowing it to accelerate quickly, primates (and humans) can ultimately achieve faster movements due to their longer and more powerful legs and necks (Gould, 1974). Since vestibular afferents in rodents and monkeys displayed similar levels of variability (Sadeghi *et al.* 2007; Lasker *et al.* 2008), the observed lower neuronal sensitivities of vestibular neurons in mice would be disadvantageous for coding (Swets *et al.* 1978; Vinje

& Gallant, 2000; Borst & Haag, 2001). One alternative possibility is that in the mouse information from the highly sensitive vibrissae system, which is not found in monkeys and humans, provides essential self-motion cues that are combined with vestibular information to improve the accuracy of head motion tracking during locomotion (Sofroniew & Svoboda, 2015; Sofroniew *et al.* 2015). Further studies will be required to establish whether this hypothesis is correct.

Overall, our results showing fundamental differences in natural self-motion statistics across species are expected to have important implications for choosing animal models for studying vestibular processing. While we found some differences between the statistics of self-motion stimuli experienced by monkeys and humans, these were more similar to one another than to those experienced by mice. Our results therefore suggest that the coding strategies used to process natural self-motion by the vestibular systems of monkeys and humans will more closely resemble one another than those used by the vestibular system of mice.

Implications for other systems

As noted above, the natural stimuli experienced by the vestibular system appear to be fundamentally different from those observed for other modalities because their spectral power does not generally follow a power law. This is the case for the rotational motion experienced by all mammalian species tested to date, as well as for the translational motion experienced by monkeys and humans. Thus, our results bring forward the important question of whether the vestibular system employs neural coding strategies that are fundamentally different from those of other sensory systems. Put another way, are the coding strategies used by the vestibular system optimized to the unique spectral structure of the signals (i.e. shaped by biomechanics and active motion) impinging on the sensors in the head? Indeed, the adaptation of vestibular pathways to stimuli that do not follow a power law would have important consequences for higher levels of processing. Notably, Weber's law, which states that the discrimination threshold is proportional to stimulus magnitude, is observed across sensory systems (Laming, 1986; Zanker, 1996; Dehaene, 2003; Brannon *et al.* 2008; Francisco *et al.* 2008). The fact that sensory perception follows Weber's law is commonly thought to be a consequence of adaptation of the coding strategies used by sensory systems to natural stimuli with spectral power that follows a power law (Shepard, 1987; Anderson, 1990; Chater & Brown, 1999). Thus, if our prediction is correct, then vestibular perception should deviate from Weber's law. While some studies suggest that vestibular perception does indeed follow Weber's law for translational stimuli (Naseri & Grant, 2012), others instead suggest a deviation

from Weber's law for rotational stimuli (Mallery *et al.* 2010). However, as both studies only tested relatively low (≤0.6 Hz) frequencies, experiments testing vestibular perception over the natural frequency range (0–20 Hz) are necessary to test whether vestibular perception does not follow Weber's law.

Future studies will also be required to further our understanding of how behaviour shapes the encoding of sensory stimuli. In natural conditions, the vestibular stimuli experienced by mice and monkeys are actively generated. Interestingly, recent studies have shown that active sensing can contribute to shaping the structure of natural visual, somatosensory, and vestibular stimuli prior to sensory transduction (Kuang *et al.* 2012; Moore *et al.* 2013; Carriot *et al.* 2014). For example, the observation that mice minimize their vertical head motion during self-motion (e.g. Pozzo *et al.* 1991*a,b*; Bril & Ledebt, 1998; Cromwell *et al.* 2002, 2004*a,b*) effectively constrains the structure of natural vestibular stimuli. We speculate that this will in turn alter the coding strategy used to represent vertical motion. Indeed, we hypothesize that combined effects of active sensing and biomechanics alter the statistics of natural signals in other sensory modalities prior to sensory transduction, suggesting that additional studies in behaving animals are required to fully establish the fundamental properties that determine the neural code. In addition, future studies should focus on the statistics of the vestibular input during self-motion for different age groups as well as across gender. In the present study, we focused on head motion in adult male monkeys and mice. Normative data sets that include a broad range of age groups across gender would facilitate comparisons with different experimental groups (e.g. maturation in different natural environments, normal *versus* transgenic animals, or animals with specific central nervous system lesions) to establish whether and how the statistics of natural vestibular stimuli change.

References

Alagramam KN, Stahl JS, Jones SM, Pawlowski KS & Wright CG (2005). Characterization of vestibular dysfunction in the mouse model for Usher syndrome 1F. *J Assoc Res Otolaryngol* **6**, 106–118.

Alonso PD, Milner AC, Ketcham RA, Cookson MJ & Rowe TB (2004). The avian nature of the brain and inner ear of Archaeopteryx. *Nature* **430**, 666–669.

Anderson JR (1990). *The Adaptive Character of Thought*. Erlbaum, Hillsdale, NJ, USA.

Attneave F (1954). Some informational aspects of visual perception. *Psychol Rev* **61**, 183–193.

Bagnall MW, Stevens RJ & du Lac S (2007). Transgenic mouse lines subdivide medial vestibular nucleus neurons into discrete, neurochemically distinct populations. *J Neurosci* **27**, 2318–2330.

Barlow H (2001). Redundancy reduction revisited. *Network* **12**, 241–253.

Barlow HB, Narasimhan R & Rosenfeld A (1972). Visual pattern analysis in machines and animals. *Science* **177**, 567–575.

Beraneck M & Cullen KE (2007). Activity of vestibular nuclei neurons during vestibular and optokinetic stimulation in the alert mouse. *J Neurophysiol* **98**, 1549–1565.

Borst A & Haag J (2001). Effects of mean firing on neural information rate. *J Comput Neurosci* **10**, 213–221.

Brannon EM, Libertus ME, Meck WH & Woldorff MG (2008). Electrophysiological measures of time processing in infant and adult brains: Weber's Law holds. *J Cogn Neurosci* **20**, 193–203.

Bril B & Ledebt A (1998). Head coordination as a means to assist sensory integration in learning to walk. *Neurosci Biobehav Rev* **22**, 555–563.

Carriot J, Jamali M, Chacron MJ & Cullen KE (2014). Statistics of the vestibular input experienced during natural self-motion: implications for neural processing. *J Neurosci* **34**, 8347–8357.

Chater N & Brown GD (1999). Scale-invariance as a unifying psychological principle. *Cognition* **69**, B17–24.

Clarke AH (2005). On the vestibular labyrinth of *Brachiosaurus brancai*. *J Vestib Res* **15**, 65–71.

Cromwell R, Schurter J, Shelton S & Vora S (2004*a*). Head stabilization strategies in the sagittal plane during locomotor tasks. *Physiother Res Int* **9**, 33–42.

Cromwell RL, Newton RA & Forrest G (2002). Influence of vision on head stabilization strategies in older adults during walking. *J Gerontol A Biol Sci Med Sci* **57**, M442–448.

Cromwell RL, Pidcoe PE, Griffin LA, Sotillo T, Ganninger D & Feagin M (2004*b*). Adaptations in horizontal head stabilization in response to altered vision and gaze during natural walking. *J Vestib Res* **14**, 367–373.

Cullen KE (2012). The vestibular system: multimodal integration and encoding of self-motion for motor control. *Trends Neurosci* **35**, 185–196.

Cullen KE, Chen-Huang C & McCrea RA (1993). Firing behavior of brain stem neurons during voluntary cancellation of the horizontal vestibuloocular reflex. II. Eye movement related neurons. *J Neurophysiol* **70**, 844–856.

Cullen KE & McCrea RA (1993). Firing behavior of brain stem neurons during voluntary cancellation of the horizontal vestibuloocular reflex. I. Secondary vestibular neurons. *J Neurophysiol* **70**, 828–843.

Dan Y, Atick JJ & Reid RC (1996). Efficient coding of natural scenes in the lateral geniculate nucleus: experimental test of a computational theory. *J Neurosci* **16**, 3351–3362.

Dehaene S (2003). The neural basis of the Weber-Fechner law: a logarithmic mental number line. *Trends Cogn Sci* **7**, 145–147.

Francisco E, Tannan V, Zhang Z, Holden J & Tommerdahl M (2008). Vibrotactile amplitude discrimination capacity parallels magnitude changes in somatosensory cortex and follows Weber's Law. *Exp Brain Res* **191**, 49–56.

Gould SJ (1974). Size and shape. *Natural History Magazine* **83**, 20–36.

Graf W, de Waele C & Vidal PP (1995). Functional anatomy of the head-neck movement system of quadrupedal and bipedal mammals. *J Anat* **186**, 55–74.

Hinz B, Menzel G, Bluthner R & Seidel H (2010). Seat-to-head transfer function of seated men – determination with single and three axis excitations at different magnitudes. *Ind Health* **48**, 565–583.

Hoebeek FE, Stahl JS, van Alphen AM, Schonewille M, Luo C, Rutteman M, van den Maagdenberg AM, Molenaar PC, Goossens HH, Frens MA & De Zeeuw CI (2005). Increased noise level of Purkinje cell activities minimizes impact of their modulation during sensorimotor control. *Neuron* **45**, 953–965.

Huang CG, Zhang ZD & Chacron MJ (2016). Temporal decorrelation by SK channels enables efficient neural coding and perception of natural stimuli. *Nat Commun* **7**, 11353.

Jones GM & Spells KE (1963). A theoretical and comparative study of the functional dependence of the semicircular canal upon its physical dimensions. *Proc R Soc Lond B Biol Sci* **157**, 403–419.

Jones SM & Jones TA (2014). Genetics of peripheral vestibular dysfunction: lessons from mutant mouse strains. *J Am Acad Audiol* **25**, 289–301.

Kuang X, Poletti M, Victor JD & Rucci M (2012). Temporal encoding of spatial information during active visual fixation. *Curr Biol* **22**, 510–514.

Laming D (1986). *Sensory Analysis.* Academic Press, London.

Lasker DM, Han GC, Park HJ & Minor LB (2008). Rotational responses of vestibular-nerve afferents innervating the semicircular canals in the C57BL/6 mouse. *J Assoc Res Otolaryngol* **9**, 334–348.

Laughlin S (1981). A simple coding procedure enhances a neurons information capacity. *Z Naturforsch C* **36**, 910–912.

Lewen GD, Bialek W & de Ruyter van Steveninck RR (2001). Neural coding of naturalistic motion stimuli. *Network* **12**, 317–329.

Luebke AE, Holt JC, Jordan PM, Wong YS, Caldwell JS & Cullen KE (2014). Loss of α-calcitonin gene-related peptide (αCGRP) reduces the efficacy of the vestibulo-ocular reflex (VOR). *J Neurosci* **34**, 10453–10458.

McElvain LE, Bagnall MW, Sakatos A & du Lac S (2010). Bidirectional plasticity gated by hyperpolarization controls the gain of postsynaptic firing responses at central vestibular nerve synapses. *Neuron* **68**, 763–775.

Machens CK, Stemmler MB, Prinz P, Krahe R, Ronacher B & Herz AV (2001). Representation of acoustic communication signals by insect auditory receptor neurons. *J Neurosci* **21**, 3215–3227.

McMahon TA (1984). *Muscles, Reflexes, and Locomotion.* Princeton University Press.

Mallery RM, Olomu OU, Uchanski RM, Militchin VA & Hullar TE (2010). Human discrimination of rotational velocities. *Exp Brain Res* **204**, 11–20.

Medrea I & Cullen KE (2013). Multisensory integration in early vestibular processing in mice: the encoding of passive vs. active motion. *J Neurophysiol* **110**, 2704–2717.

Moore JD, Deschenes M, Furuta T, Huber D, Smear MC, Demers M & Kleinfeld D (2013). Hierarchy of orofacial rhythms revealed through whisking and breathing. *Nature* **497**, 205–210.

Naseri AR & Grant PR (2012). Human discrimination of translational accelerations. *Exp Brain Res* **218**, 455–464.

Nigg BM & Liu W (1999). The effect of muscle stiffness and damping on simulated impact force peaks during running. *J Biomech* **32**, 849–856.

Pozzo T, Berthoz A, Lefort L & Vitte E (1991*a*). Head stabilization during various locomotor tasks in humans. II. Patients with bilateral peripheral vestibular deficits. *Exp Brain Res* **85**, 208–217.

Pozzo T, Berthoz A, Vitte E & Lefort L (1991*b*). Head stabilization during locomotion. Perturbations induced by vestibular disorders. *Acta Otolaryngol Suppl* **481**, 322–327.

Pozzorini C, Naud R, Mensi S & Gerstner W (2013). Temporal whitening by power-law adaptation in neocortical neurons. *Nat Neurosci* **16**, 942–948.

Rieke F, Bodnar DA & Bialek W (1995). Naturalistic stimuli increase the rate and efficiency of information transmission by primary auditory afferents. *Proc Biol Sci* **262**, 259–265.

Rodriguez FA, Chen C, Read HL & Escabi MA (2010). Neural modulation tuning characteristics scale to efficiently encode natural sound statistics. *J Neurosci* **30**, 15969–15980.

Sadeghi SG, Goldberg JM, Minor LB & Cullen KE (2009). Effects of canal plugging on the vestibuloocular reflex and vestibular nerve discharge during passive and active head rotations. *J Neurophysiol* **102**, 2693–2703.

Sadeghi SG, Minor LB & Cullen KE (2007). Response of vestibular-nerve afferents to active and passive rotations under normal conditions and after unilateral labyrinthectomy. *J Neurophysiol* **97**, 1503–1514.

Schlecker C, Praetorius M, Brough DE, Presler RG Jr, Hsu C, Plinkert PK & Staecker H (2011). Selective atonal gene delivery improves balance function in a mouse model of vestibular disease. *Gene Ther* **18**, 884–890.

Schmidt M (2008). Forelimb proportions and kinematics: how are small primates different from other small mammals? *J Exp Biol* **211**, 3775–3789.

Schneider AD, Jamali M, Carriot J, Chacron MJ & Cullen KE (2015). The increased sensitivity of irregular peripheral canal and otolith vestibular afferents optimizes their encoding of natural stimuli. *J Neurosci* **35**, 5522–5536.

Shepard RN (1987). Toward a universal law of generalization for psychological science. *Science* **237**, 1317–1323.

Simoncelli EP & Olshausen BA (2001). Natural image statistics and neural representation. *Annu Rev Neurosci* **24**, 1193–1216.

Sofroniew NJ & Svoboda K (2015). Whisking. *Curr Biol* **25**, R137–140.

Sofroniew NJ, Vlasov YA, Andrew Hires S, Freeman J & Svoboda K (2015). Neural coding in barrel cortex during whisker-guided locomotion. *Elife* **4**, e12559.

Spoor F, Bajpai S, Hussain ST, Kumar K & Thewissen JG (2002). Vestibular evidence for the evolution of aquatic behaviour in early cetaceans. *Nature* **417**, 163–166.

Spoor F, Garland T Jr, Krovitz G, Ryan TM, Silcox MT & Walker A (2007). The primate semicircular canal system and locomotion. *Proc Natl Acad Sci USA* **104**, 10808–10812.

Spoor F, Wood B & Zonneveld F (1994). Implications of early hominid labyrinthine morphology for evolution of human bipedal locomotion. *Nature* **369**, 645–648.

Straka H, Zwergal A & Cullen KE (2016). Vestibular animal models: contributions to understanding physiology and disease. *J Neurol* **263**, 10–23.

Swets JA, Green DM, Getty DJ & Swets JB (1978). Signal detection and identification at successive stages of observation. *Percept Psychophys* **23**, 275–289.

Vidal PP, Degallaix L, Josset P, Gasc JP & Cullen KE (2004). Postural and locomotor control in normal and vestibularly deficient mice. *J Physiol* **559**, 625–638.

Vinje WE & Gallant JL (2000). Sparse coding and decorrelation in primary visual cortex during natural vision. *Science* **287**, 1273–1276.

Vinje WE & Gallant JL (2002). Natural stimulation of the nonclassical receptive field increases information transmission efficiency in V1. *J Neurosci* **22**, 2904–2915.

Wakeling JM, Liphardt AM & Nigg BM (2003). Muscle activity reduces soft-tissue resonance at heel-strike during walking. *J Biomech* **36**, 1761–1769.

Wakeling JM, Nigg BM & Rozitis AI (2002). Muscle activity damps the soft tissue resonance that occurs in response to pulsed and continuous vibrations. *J Appl Physiol* **93**, 1093–1103.

Wark B, Lundstrom BN & Fairhall A (2007). Sensory adaptation. *Curr Opin Neurobiol* **17**, 423–429.

Watt HJ (1924). Dimensions of the labyrinth correlated. *Proc R Soc Lond B Biol Sci* **96**, 334–338.

Zanker JM (1996). On the elementary mechanism underlying secondary motion processing. *Philos Trans R Soc Lond B Biol Sci* **351**, 1725–1736.

Zatiorsky VM (1998). *Kinematic of Human Motion.* Human Kinetics.

Additional information

Competing interests

No competing interests declared.

Author contributions

J.C.: conception and design; collection and assembly of data; data analysis and interpretation; manuscript writing; final approval of manuscript (required) M.J.: conception and design; collection and assembly of data; data analysis and interpretation; manuscript writing; final approval of manuscript (required) M.C.: Conception And Design; Data Analysis And Interpretation; Manuscript Writing; Final Approval Of Manuscript (Required) K.C.: conception and design; data analysis and interpretation; manuscript writing; final approval of manuscript (required). All authors agree to be accountable for all aspects of the work in ensuring that questions related to the accuracy or integrity of any part of the work are appropriately investigated and resolved. All persons designated as authors qualify for authorship, and all those who qualify for authorship are listed.